

Enhanced Sensitivity in Electron-Nuclear Double Resonance (ENDOR) by Cross Polarisation and Relaxation

Roberto Rizzato^a and Marina Bennati^{a,b}

^aResearch Group EPR Spectroscopy, Max Planck Institute for Biophysical Chemistry, Am Fassberg 11, 37077 Göttingen, Germany Fax: (+49) 551 201 1383; Tel. (+49) 551 201 1911

^bDepartment of Chemistry, University of Göttingen, Tammanstr. 2, 37077 Göttingen.

SI1. Master equations for ENDOR relaxation in a two-spin system in high temperature approximation

SI2. Measurement of T_{1I} at 34 and 94 GHz: Davies ENDOR spectrum as a function of t_R .

SI3. Global fit of W-band data

SI4. Simulated CP-ENDOR intensities as a function of the number of shots

SI1. Master equations for ENDOR relaxation in a two-spin system in high T approximation

In the high temperature approximation the transition probabilities between a pair of level i and j are the same in both directions, i.e. $w_{ij} = w_{ji}$. The distribution of populations N_i at each time point can be calculated by solving the rate equations (Solomon, Phys. Rev. Vol. 99, p.559, 1955):

$$\frac{d}{dt} \begin{pmatrix} N_1 \\ N_2 \\ N_3 \\ N_4 \end{pmatrix} = \begin{pmatrix} -w_a & w_{1I} & w_{1S} & w_0 \\ w_{1I} & -w_b & w_2 & w_{1S} \\ w_{1S} & w_2 & -w_b & w_{1I} \\ w_0 & w_{1S} & w_{1I} & -w_a \end{pmatrix} \begin{pmatrix} N_1 - N_1^0 \\ N_2 - N_2^0 \\ N_3 - N_3^0 \\ N_4 - N_4^0 \end{pmatrix} \quad (\text{S1})$$

with the definitions $w_a = w_{1I} + w_{1S} + w_0$ and $w_b = w_{1I} + w_{1S} + w_2$. N_i^0 indicate the populations at thermal equilibrium and w_0 , w_2 are the probabilities of the forbidden zero and double quantum transitions.

In order to reduce the system of equations, it is convenient to transform (1) by introducing a set of four new variables defined as:

$$\begin{aligned} n_S &= (N_1 - N_3) + (N_2 - N_4) = n_{S\alpha} + n_{S\beta}; \\ n_I &= (N_1 - N_2) + (N_3 - N_4) = n_{I12} + n_{I34}; \end{aligned} \quad (\text{S2})$$

$$n_{\Delta} = (N_1 - N_2) - (N_3 - N_4) = n_{I12} - n_{I34};$$

$$N = N_1 + N_2 + N_3 + N_4$$

Where $n_{I12,34}$ and $n_{S\alpha,\beta}$ refer to the population difference of the EPR and ENDOR transitions as defined in Fig. 1b. Expressed with the new variables, the system gets the well-known form of the Solomon equations:

$$\frac{d}{dt} \begin{pmatrix} N \\ n_I \\ n_S \\ n_{\Delta} \end{pmatrix} = - \begin{pmatrix} 0 & 0 & 0 & 0 \\ 0 & R_I & R_x & 0 \\ 0 & R_x & R_S & 0 \\ 0 & 0 & 0 & R_{\Delta} \end{pmatrix} \begin{pmatrix} N \\ n_I - n_I^0 \\ n_S - n_S^0 \\ n_{\Delta} \end{pmatrix} \quad (S3)$$

with the relaxation rates R defined as:

$$R_S = \frac{1}{T_{1S}} = w_2 + 2w_{1S} + w_0 \quad R_{\Delta} = \frac{1}{T_{1\Delta}} = 2w_{1S} + 2w_{1I}$$

$$R_I = \frac{1}{T_{1I}} = w_2 + 2w_{1I} + w_0 \quad R_x = \frac{1}{T_{1x}} = w_2 - w_0 \quad (S4)$$

The general solution is given by:

$$n_I(t) = c_1 e^{\lambda_1 t} + c_2 e^{\lambda_2 t} + n_I^B$$

$$n_S(t) = c_3 e^{\lambda_1 t} + c_4 e^{\lambda_2 t} + n_S^B \quad (S5)$$

$$n_{\Delta}(t) = n_{0\Delta} e^{R_{\Delta} t}$$

With the exponents: $\lambda_{1,2} = \frac{1}{2} \left[-(R_I + R_S) \pm \sqrt{(R_I - R_S)^2 + 4R_x^2} \right]$.

n_I^B and n_S^B are the nuclear and electron Boltzmann polarizations. Considering the electron Zeeman as the dominant interaction $\omega_{0S} \gg \omega_{0I}$ we set $n_{S\alpha}^B \approx n_{S\beta}^B \equiv n_S^B$ and neglect the nuclear spin Boltzmann polarization, $n_{I,12}^B = n_{I,34}^B = 0$, in eq. S3 and the subsequent ones.

Assuming that the difference between electron and nuclear spin transition rates is much greater than between the two forbidden cross transition rates: $|w_{1I} - w_{1S}| \gg |w_2 - w_0| \Rightarrow |R_I - R_S| \gg R_x$ the two exponents simplify to:

$$\lambda_1 = -R_S = -\frac{1}{T_{1S}} \quad \lambda_2 = -R_I = -\frac{1}{T_{1I}} \quad (S6)$$

Thus the exponents reduce to the electron-spin lattice and nuclear-spin lattice relaxation rate, respectively. The coefficients of eq. S5 depend on the initial conditions, i.e. the polarization at begin ($t = 0$) of the observed time evolution. We used Mathematica (Wolfram Research, Inc.) to solve the system and simplify the solutions, finally we obtain for the ENDOR lines (eq. 1 in the main text):

$$\begin{aligned}
n_{I12}(t) &= \frac{1}{4} \left(2e^{-tR_I} (n_{0I12} + n_{0I34}) + 2e^{-tR_\Delta} n_{0\Delta} \right) \\
n_{I34}(t) &= \frac{1}{4} \left(2e^{-tR_I} (n_{0I12} + n_{0I34}) - 2e^{-tR_\Delta} n_{0\Delta} \right)
\end{aligned} \tag{S7}$$

and the polarization of the EPR lines gets the form:

$$\begin{aligned}
n_{S\alpha}(t) &= \frac{1}{4} \left(4n_{BS} + 2e^{-tR_S} (-2n_{BS} + n_{0S\beta} + n_{0S\alpha}) + 2e^{-tR_\Delta} n_{0\Delta} \right) \\
n_{S\beta}(t) &= \frac{1}{4} \left(4n_{BS} + 2e^{-tR_S} (-2n_{BS} + n_{0S\beta} + n_{0S\alpha}) - 2e^{-tR_\Delta} n_{0\Delta} \right)
\end{aligned} \tag{S8}$$

We stress here that the coefficients $n_{0I,12}$ and $n_{0I,34}$ in equation S7 (or eq. 1 main text) and correspondingly in eq. S8 are not the Boltzmann factors but the population differences at begin of the observed time evolution.

SI2. Measurement of T_{11} at 34 and 94 GHz: Davies ENDOR spectrum as a function of t_R .

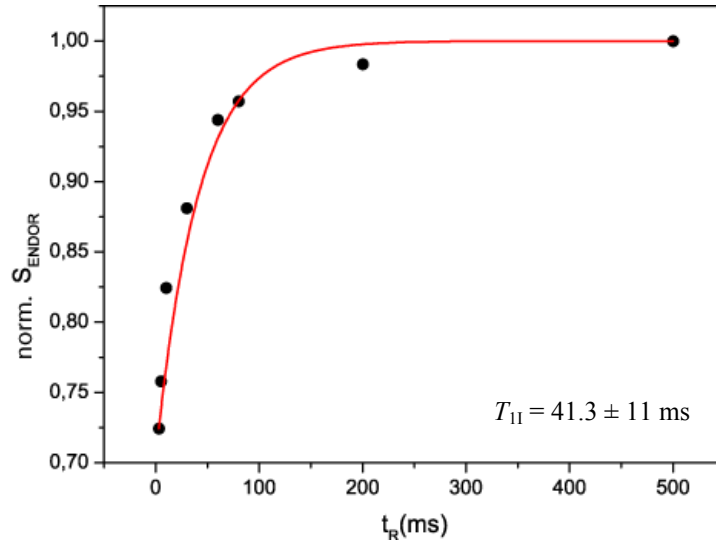


Figure S1: Intensity of the Davies ENDOR line at + 2.5 MHz as a function of the repetition time t_r . Exp. conditions: $\nu_{\text{mw}}=34$ GHz, $T=20$ K, $\pi_{\text{mw}}: 200$ ns, $\pi_{\text{rf}} = 15$ us, 10 shots per point, 1 scan.

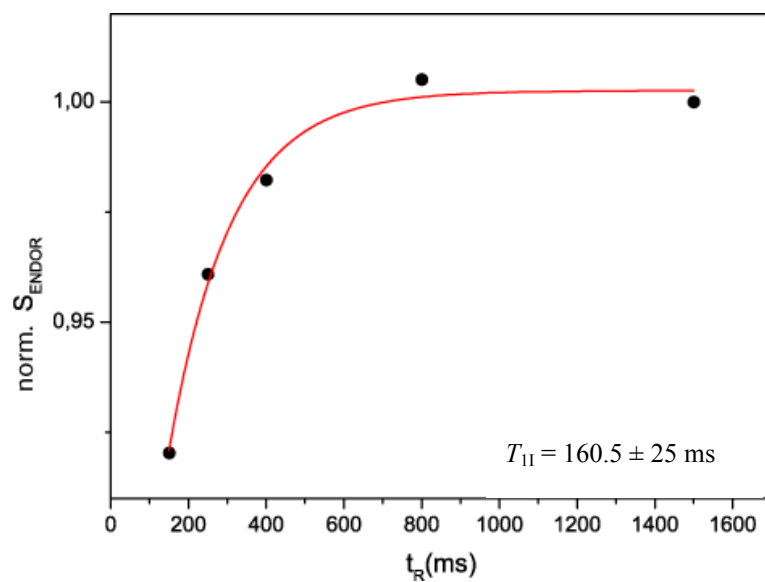


Figure S2: Intensity of the Davies ENDOR line at + 2.5 MHz as a function of the repetition time t_r . Exp. conditions: $\nu_{\text{mw}}=94$ GHz, $T=50$ K, π_{mw} : 200 ns, $\pi_{\text{rf}}=25$ us, 10 shots per point, 1 scan.

SI3. Global fit of W-band data

In an attempt to rationalize the discrepancy between the fitted τ_1 and the T_{1S} values in the W-band data (Fig. 3b and Table 1), a global model has been utilized, which considers the two datasets of the decay curves at $\Delta\omega_h^{\text{ENDOR}} = +2.5$ MHz and -2.5 MHz simultaneously. The model fits the four amplitudes as independent quantities and the two rates as common parameters. The fitted values are reported in Table S1. We observe that the new value for τ_1 lies between the values of 4 and 15 ms found by the individual fits in Fig. 3. The error $\Delta\tau_1$ also reflects this range of values. Therefore, the difference in τ_1 seems to reflect a real behavior of the curve. This difference might be due to different spectral diffusion effects at the two spectral positions of the ENDOR line.

The global fit also underestimates the second time constant τ_2 , as visible also on Figure S3. Therefore, we conclude that the independent fit of the two decay curves with values in Table 1 is closer to the experimental values.

$\nu_{\text{mw}} = 94 \text{ GHz}$	A_1	$\tau_1 \text{ (ms)}$	$\Delta\tau_1 \text{ (ms)}$	A_2	$\tau_2 \text{ (ms)}$	$\Delta\tau_2 \text{ (ms)}$
ENDOR line: + 2.5MHz	$+0.50 \pm 0.15$	7	5 to 13	$+0.47 \pm 0.15$	69	49 to 114
ENDOR line: - 2.5MHz	$+0.31 \pm 0.25$	7	5 to 13	-0.27 ± 0.25	69	49 to 114

Table S1: Parameters of the global fit for the kinetic curves of Fig 3b. $\Delta\tau$ represents the error given by the fit.

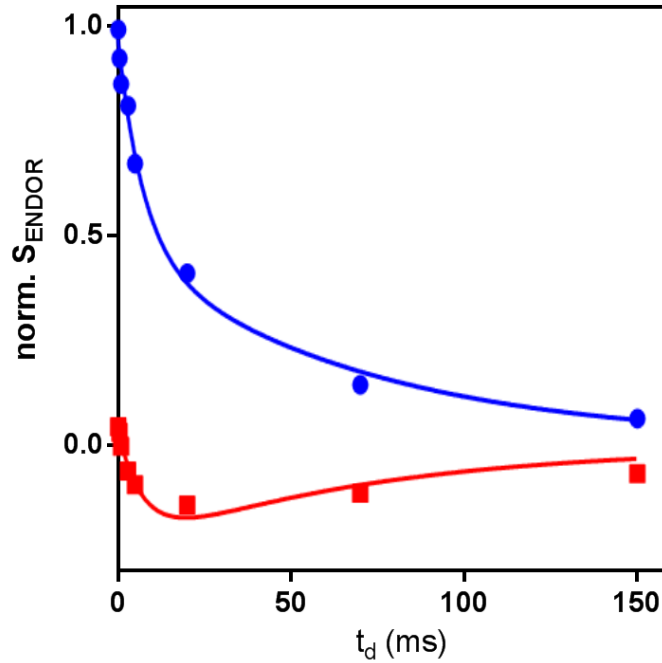


Figure S3: Global nonlinear fit of the intensity of the CP-ENDOR lines at $\Delta\omega_h^{\text{ENDOR}} = + 2.5$ MHz (blue) and -2.5 MHz (red) as a function of t_d at 94 GHz, $T = 50$ K

SI4. Simulated CP-ENDOR intensities as a function of the number of shots

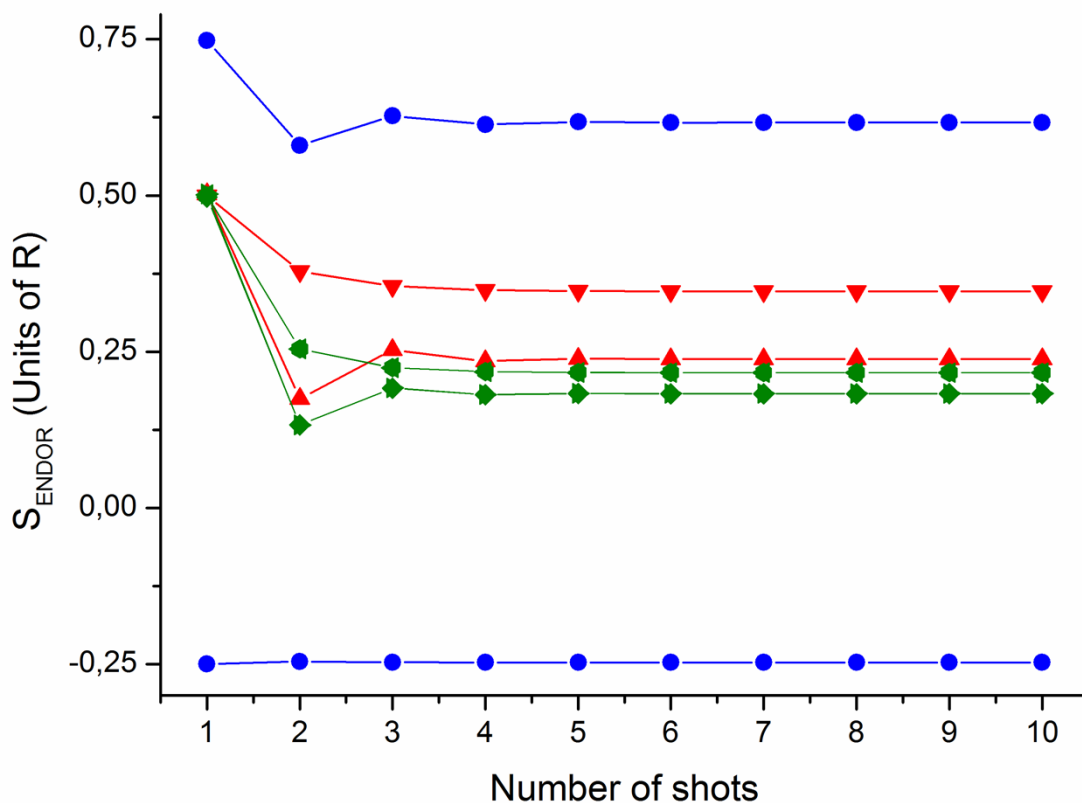


Figure S4: Numerical simulations for the intensities of the ENDOR lines 12 (dots) and 34 (triangles) in the asymmetric CP-ENDOR (blue), the symmetric CP-ENDOR (red) and residual ENDOR (CP with RF off) as a function of the number of shots (repetitions of the sequence). Parameters: $\nu_{\text{EPR}} = 94$ GHz, $T = 5$ K, $t_r = T_{1S}$, $T_{1I} = T_{1x} = 10 \cdot T_{1S}$.